Hindawi
Journal of Sensors
Volume 2021, Article ID 7294604, 10 pages
https://doi.org/10.1155/2021/7294604

Research Article

A Method of UWB Radar Vital Detection Based on P Time Extraction of Strong Vital Signs

Zhen Yang,[1] **Jiming Cheng**,[1] **Qingjie Qi**,[2] **Xin Li**,[1] **and Yuning Wang**[1]

[1]*Faculty of Electrical and Control Engineering, Liaoning Technical University, Huludao 125105, China*
[2]*Emergency Research Institute, China Coal Research Institute CCRI, Beijing 100000, China*

Correspondence should be addressed to Jiming Cheng; chjm0527@126.com

Received 27 June 2021; Accepted 23 August 2021; Published 20 September 2021

Academic Editor: Antonio Lazaro

The vital sign information in the echo signal of the UWB radar is weak, because of the interference of complex noise. In this paper, a method named P times extraction of strong vital signs for processing echo signals of UWB radars is proposed. Different noises can be distinguished by the cumulative probability distribution of the echo signal and using different methods for processing according to corresponding characteristics. The vital sign information which most clearly represents the trapped person is selected using P times extraction of strong vital signs; then, the respiration and heartbeat rates are extracted. At 5 different distances, multiple sets of tests were carried out on static trapped persons and micromovement trapped persons and using a computer to extract vital signs from the obtained data. Experimental data shows that the algorithm proposed in this paper can extract the respiration and heartbeat rates of trapped persons, with small relative errors and variances, and has a certain reference value for UWB radar signal processing.

1. Introduction

The vital detection using a radar has broad application prospects in both military and civilian use, such as search and rescue of the wounded on the battlefield after the war, the search for survivors in the rubble after an earthquake or landslide, and patient monitoring during medical procedures [1–3]. Currently, two main types of radars are used for noncontact vital signal detection: continuous wave radar and UWB radar [4]. Continuous wave radar has been used for this purpose [5, 6], which has the advantages of simple structure, strong frequency domain recognition ability, and simple signal processing [7]. But it can only obtain the Doppler frequency information of the target, not distance information. Compared with the Doppler radar, the UWB radar can not only obtain the distance and frequency information of the trapped person at the same time but also has a great improvement in penetration ability, anti-interference ability, resolution, and power consumption [8, 9]. These advantages ensure the accuracy and sensitivity of the radar echo signal. Therefore, the UWB radar has gradually become the main application technology in the field of vital detection and monitoring and its echo signal preprocessing methods and vital sign extraction methods have gradually become research hotspots.

When performing vital sign detection, the signal-to-noise ratio (SNR) of the echo signal is low [10–12], because the signal received by the radar contains not only the target reflection echo but also a large amount of complex noise. References [13, 14] used their own algorithms to process the echo signals and achievements have been made in improving the SNR. Reference [15] used the vital sign monitoring method of Nth peak capture to filter out clutter and noise, extract the respiration rate, and suppress its higher harmonics. Reference [16] proposed an UWB radar signal processing method with periodic sampling and superposition, which transfers the frequency information to the baseband and avoids the information loss caused by the dispersion of the spectrum. Reference [17] used singular value decomposition (SVD) to eliminate the noise in the vital signal and used FFT and Hilbert-Huang transform to extract the vital signs. Reference [18] used empirical mode

decomposition (EMD) to decompose the radar echo signal, selecting intrinsic mode function (IMF) for reconstruction to obtain the respiration and heartbeat rates. References [19–21] made improvements on the basis of the EMD and achieved certain results of processing the UWB radar echo signals.

In the algorithm proposed above, the basis of vital signs detected is one or more slow-time slices containing vital signs. However, in the case of complex noise interference, the vital signs contained in a single slow-time slice are weak, which is vulnerable to noise interference with poor stability and accuracy. What is worse is that external reasons cause the trapped person to move slightly, so the vital information contained in the selected slow-time slice is incomplete, and it is impossible to accurately obtain the trapped person's vital information. If we want to obtain complete information, the combined superposition method of multiple slices will be used. However, this method will be disturbed by other noise slices and weaken the vital signs of the trapped person and the quality of the signs obtained cannot be guaranteed.

In order to solve the above problems, an UWB radar vital information detection algorithm based on P times strong vital sign extraction is proposed. This method extracts P times vital signs from the regional echo signal that contains vital information, which obtains the most representative P group information of the trapped person. So, the method can improve the quality of the vital signs and ensure its accuracy and stability. Then, P group information of the trapped people will be parsed in the spectrum and the respiration and heartbeat rates were extracted according to the peak distribution of P group results. The accuracy and stability of the results were further guaranteed by P times different analysis.

2. Basic Principles of UWB Radar Vital Detection

The UWB radar vital detection signal is a micromotion signal of the trapped person. When the trapped person is alive, respiration and heartbeat will drive the chest to produce two different regular movements. It can be seen in Figure 1, when the radar system and the trapped person are both fixed, the distance d changes with the movement of the thoracic cavity Δd. By continuously measuring the regular of d, the vital sign information of the trapped person can be obtained.

Research shows [22], the frequency band of respiration is between 0.2 Hz–0.5 Hz, the amplitude of chest cavity movement is 5 mm–15 mm, moving area is about 50 cm^2; heartbeat frequency band is between 0.8 Hz–2.5 Hz, the amplitude change of chest cavity is about 2 mm-3 mm, moving area is about 10 cm^2. With a complex application background, the heart rate is more difficult to extract than the respiration rate.

In the process of respiration and heartbeat, the contraction and relaxation of muscles cause the cyclical fluctuations of the chest cavity, which are approximately sinusoidal. According to the basic principles of the UWB radar, the

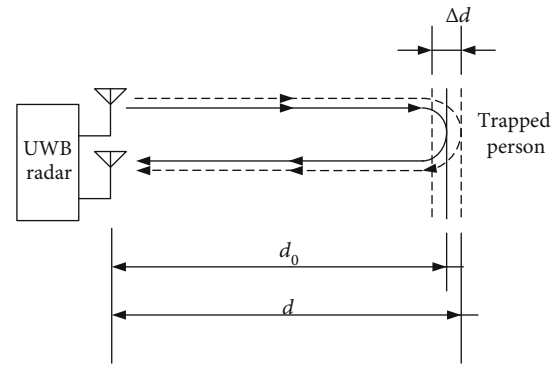

Figure 1: Schematic diagram of UWB radar vital detection. Where d_0 is the reference distance between the radar system and the trapped person, d is the actual distance, and Δd is the movement distance of the chest cavity.

instantaneous distance between the radar antenna and the trapped person chest is [23]

$$d(t) = d_0 + \Delta d = d_0 + A_r \sin(2\pi f_r t) + A_h \sin(2\pi f_h t), \quad (1)$$

where A_r and A_h are the amplitude changes of the thoracic cavity caused by respiration and heartbeat, respectively; f_r is the trapped person respiration rate, f_h is the heartbeat rate, and t is the slow time. According to equation (1), the time delay between the transmitted pulse and the received pulse can be obtained as

$$\tau_v(t) = \frac{2 \times d(t)}{v} = \tau_0 + \tau_r \sin(2\pi f_r t) + \tau_h \sin(2\pi f_h t), \quad (2)$$

where v is the speed of light in air, $\tau_r = 2A_r/v$, and $\tau_h = 2A_h/v$. With the assumption that the environment is static and the thoracic cavity of the trapped person moves periodically, this movement is manifested in a time-varying channel impulse response:

$$h(\tau, t) = a_v \delta(\tau - \tau_v(t)) + \sum_i a_i \delta(\tau - \tau_i), \quad (3)$$

where a_v and a_i are the reflection coefficients of the trapped person and the ith environmental factor to radar waves; τ_v and τ_i are the corresponding time delays of the trapped person and the ith environmental factor. The signal measured by the receive antenna can be written as the convolution of the transmit pulse and the channel impulse response:

$$r(\tau, t) = s(\tau) * h(\tau, t) = a_v s\delta(\tau - \tau_v(t)) + \sum_i a_i s\delta(\tau - \tau_i) + n(\tau, t), \quad (4)$$

where $s(\tau)$ is the first-order Gaussian pulse signal as the propagation signal, $*$ is the convolution operation, and $n(\tau, t)$ is

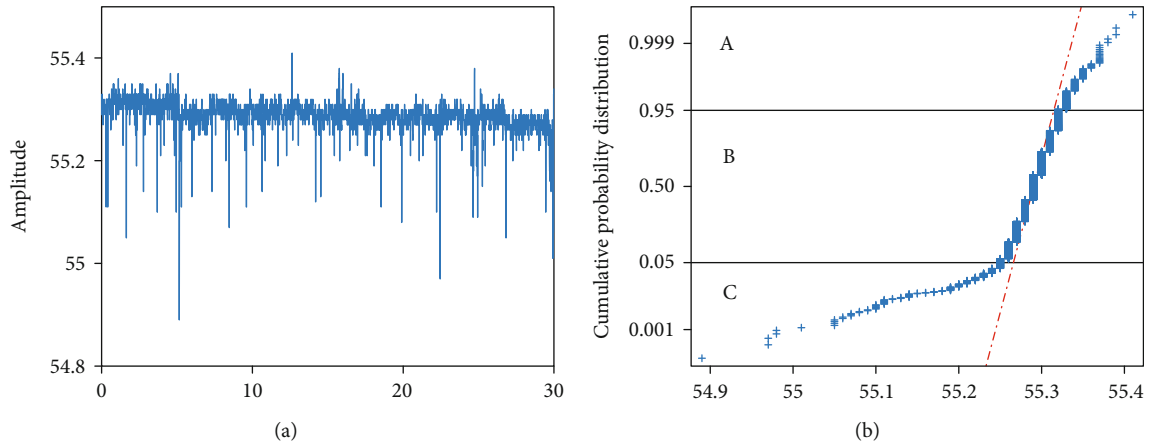

FIGURE 2: Schematic diagram of the most stable static clutter slow time slice. (a) Time domain of slow time. (b) Cumulative probability distribution chart. The red straight line in (b) is the reference normal distribution curve of all amplitudes in the slow time slice.

the random noise. Then, discrete the received signals and store it in the matrix $R[m, n]$:

$$R[m,n] = r(m\delta_T, nT_s) = a_v s(m\delta_T - \tau_v(nT_s)) + \sum_i a_i s(\tau - \tau_i) + n(m\delta_T, nT_s), \tag{5}$$

where $t = nT_s\ (n = 1, 2, \cdots, N)$ is the slow time, T_s is the sampling interval in slow time, $\tau = m\delta_T$, $(m = 1, 2, \cdots, M)$ is the fast time, and δ_T is the sampling interval in fast time.

3. Received Signal Preprocessing

3.1. Noise Analysis. In order to facilitate subsequent signal processing and improve the SNR of the signal, the received signal needs to be preprocessed before the vital signal extraction. In addition to the trapped person vital information, the received signal of the UWB radar system also includes numerous noise interferences, including static clutter, linear trend, and random noise. In order to facilitate the understanding of the distribution of various noises, the analysis based on the cumulative probability distribution of slow time slices is carried out. Choosing a slow time slice arbitrarily, then, valuate the probability of $X = x_i\ (i = 1, 2, \cdots, I)$ as $p(x_i)$, where x_i is the value appeared in the slice. The condition of amplitude distribution of all slices satisfies equation (6) as follows:

$$\sum_{i=1}^{I} p(x_i) = 1, \quad 0 \le p(x_i) \le 1. \tag{6}$$

For any X in this slice, the corresponding cumulative probability distribution function is

$$F(X) = P\{X \le x_i\}, \tag{7}$$

where $0 \le F(X) \le 1$ and $F(X)$ is a nondecreasing function of X.

Select the most stable static clutter slow time slice of the received signal, calculate its cumulative probability distribution, and draw the schematic diagram as shown in Figure 2.

Combined with equation (5), the environment of the trapped person does not change and the law of reflection and refraction of the radar signal does not change. It can be obtained that the static clutter does not change with time, which can be considered as a fixed value. Therefore, as shown in Figure 2(b), the static clutter reference value is around 55.3 and the slope of this position is larger, which means that the data is relatively concentrated. Due to the linear trend and random noise interference, the cumulative probability distribution curve of area B is consistent with the reference normal distribution curve. The prominent peak in Figure 2(a) corresponds to areas A and C in Figure 2(b), which are linear errors caused by radar instability. The error will affect the entire fast time direction, the amplitude is higher, but the frequency is lower. Random noise is mainly caused by electromagnetic interference, which is characterized by wide distribution and high frequency.

And the schematic diagram of the slow time slice containing the vital sign of the trapped person is shown in Figure 3.

The slopes of the curves in A and C regions in Figure 3(b) are larger, because A and C regions include not only linear errors but also the peak and trough values of the curve shown in Figure 3(a).

3.2. Preprocessing Methods. In view of the above noise characteristics, the following preprocessing methods are adopted.

3.2.1. Linear Error Correction. The variance of the slow-time slice can reflect the degree of deviation between the slice and its mean, and the variance of the ideal static clutter slow time slice is 0. Calculate and set the slow time slice with the minimum variance as the radar stability reference slice. By calculating the occurrence probability of the amplitude in the

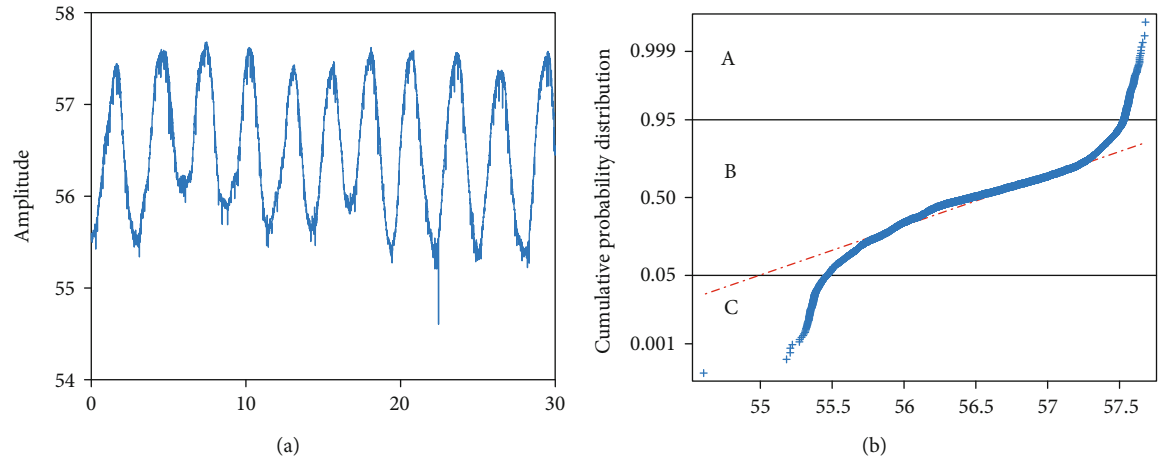

Figure 3: Schematic diagram of the slow time slice containing the vital sign of the trapped person. (a) Time domain of slow time. (b) Cumulative probability distribution chart.

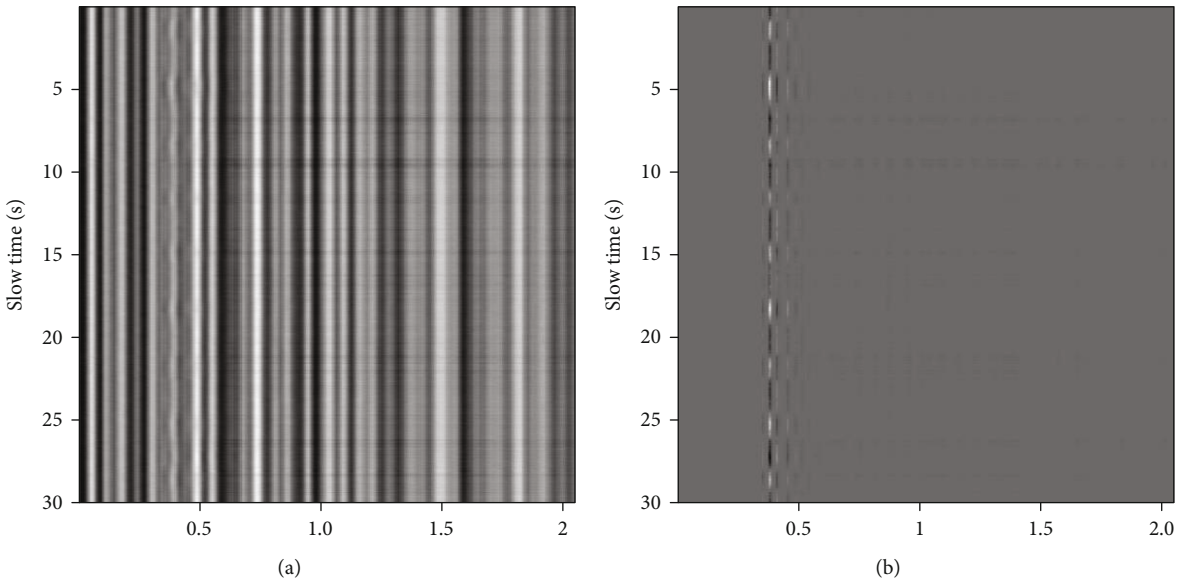

Figure 4: Preprocessing effect diagram. (a) Grayscale of the original received signal. (b) Grayscale of the received signal after preprocessing.

reference slice, it can be considered that the amplitude with the probability of occurrence less than 0.5% is caused by radar instability. Then, the fast time slice which contains unstable values is corrected according to the trend of the reference slow time slice.

3.2.2. Linear Trend Suppression. After completing the correction of the linear error, the slow time slice still has a linear trend and this problem will be solved by linear trend suppression in the slow time direction. After estimating the linear trend of the slow time slice, it is subtracted from the original slice to obtain a matrix W which does not contain static clutter and linear trend [24].

$$W^T = \Omega^T - z\left(z^T z\right)^{-1} z^T \Omega^T, \tag{8}$$

where $z = [z_1, z_2]$, $z_1 = [1, 2, \cdots, N]^T$, $z_2 = [1, 1, \cdots, 1]^T$.

3.2.3. Signal Enhancement. In practical applications, the signal received by the UWB radar system is weak due to electromagnetic interference and multipath effects. Therefore, the received signal needs to be enhanced to improve the SNR. For preserving the vital signal, the Butterworth filtering is adopted to filter out low-frequency and high-frequency interference and its bandpass frequency is 0.1 Hz–3 Hz. For the matrix obtained after the above processing, it mainly contains vital information and zero mean noise. The vital information of the trapped person has a certain periodicity, but zero-mean noise does not which can be reduced to 0 through autocorrelation [10].

$$R\left(n'\right) = E[x_m(n_1)x_m(n_2)], \tag{9}$$

where $0 \le n_1, n_2 \le N-1$, $n^{'} = n_1 - n_2$. E is for the average.

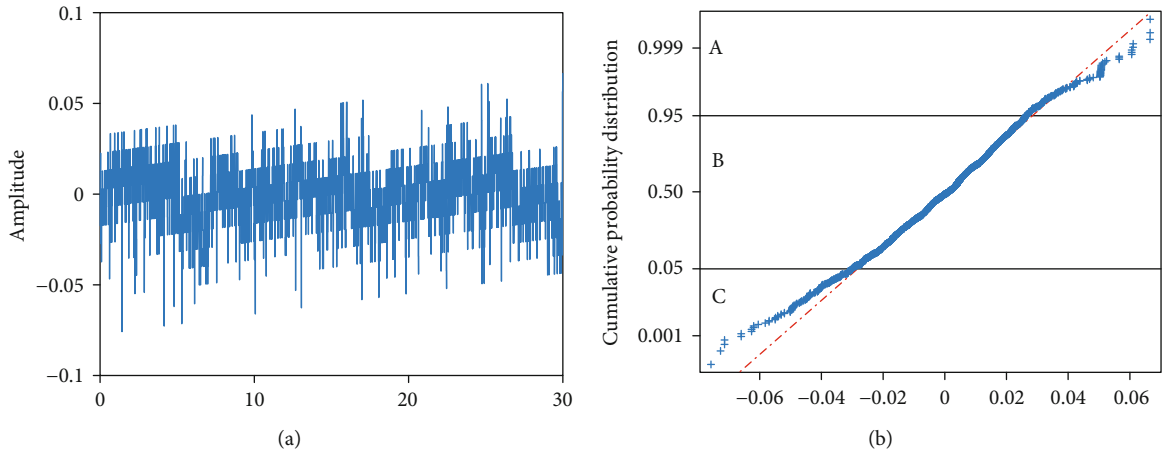

Figure 5: The schematic diagram of the static clutter slow time slice after preprocessing. (a) Time domain of slow time. (b) Cumulative probability distribution chart.

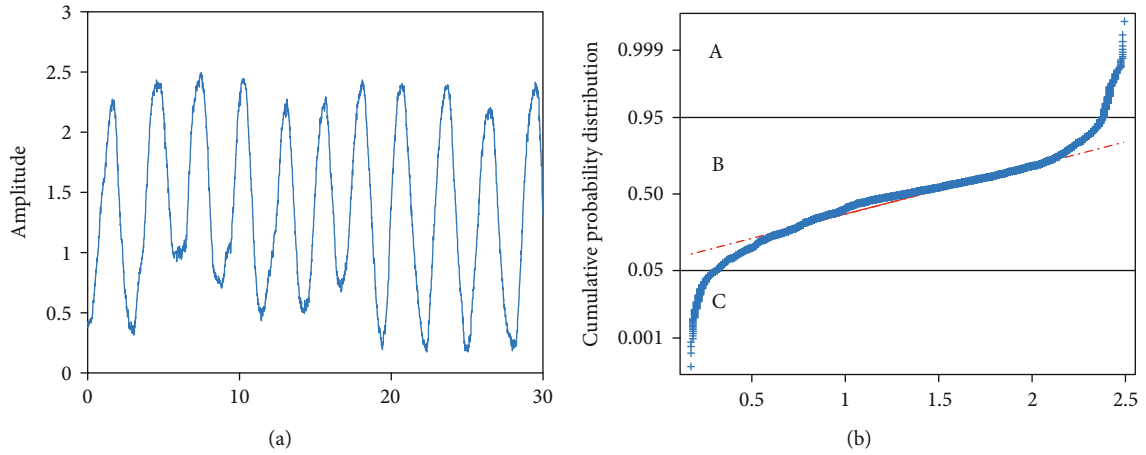

Figure 6: The schematic diagram of the slow time slice containing the vital sign of the trapped person after preprocessing. (a) Time domain of slow time. (b) Cumulative probability distribution chart.

The received signals before and after preprocessing are shown in Figure 4 to verify the effectiveness of the preprocessing methods.

The schematic diagram of the static clutter slow time slice after preprocessing is shown in Figure 5, and the slow time slice containing the vital sign of the trapped person after preprocessing is shown in Figure 6.

The vital sign information in the original signal has been drowned in noise (see Figure 4(a)). In Figure 4(b), various clutters are filtered effectively by preprocessing and the vital information of the trapped person is displayed. It can be seen in Figure 5 that in the preprocessed slow time slice, linear error, static clutter, and linear trend are all filtered out effectively and the remaining part is low-amplitude random noise with a reference value of 0. In Figure 6, with the vital signs being intact, the noise interference is effectively suppressed and the SNR is significantly improved.

4. P Times Extraction of Strong Vital Signs

Vital sign information of the trapped person is contained in multiple slow time slices. Each slice contains the respiration and heartbeat rates of the trapped person, but there are certain differences in the strength of the vital information and whether it is complete. If you only select one slow time data slice as the benchmark for vital sign extraction, it is very easy to cause the wrong estimation of vital sign information about the trapped person. What is worse is that the trapped person shakes or moves in a small distance; only one slow time slice cannot fully reflect the vital signs of the trapped person. The method of P times extraction of strong vital signs will be used to extract the respiration and heartbeat rates of the trapped person.

The energy of the slow time slice is used as the basis for the judgment of the initial search starting point. The signal energy is defined as

$$e_n = \sum_{m=1}^{M} \left| f_{(m,n)} \right|^2, \tag{10}$$

where $f(m, n)$ is the amplitude of the mth row and nth column in the matrix and e_n is the energy to the nth slow time slice. The vital sign information of the trapped person is

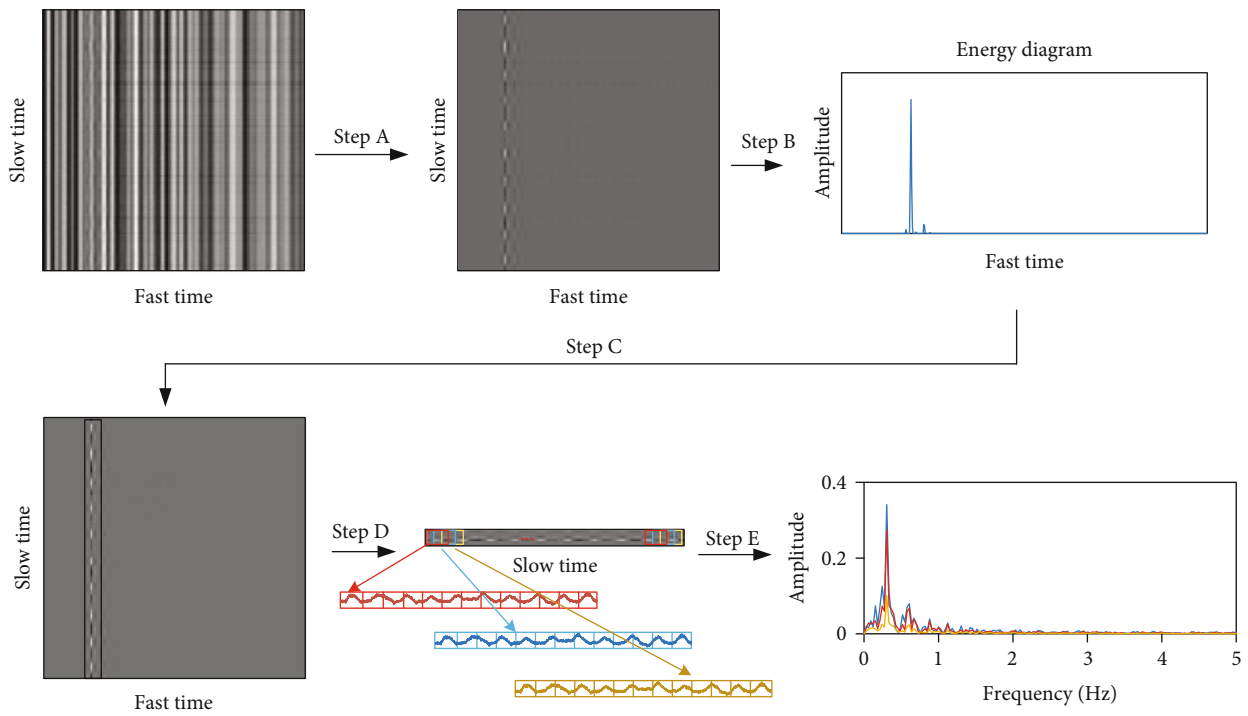

Figure 7: Flow chart of vital sign extraction, where step A is the preprocessing. Step B calculates energy from the slow time dimension and determines the maximum energy window position through step C. Step D is the process of P times extraction of strong vital signs, and finally, obtain the corresponding frequency through step E.

generally contained in 4–6 slow time slices, and an energy window with a width of 3 is used to prevent the influence of individual slow time slices on the positioning results.

$$E_n = \sum_{n-1}^{n+1} e_n, \tag{11}$$

where E_n is the energy of the nth sampling window of the received signal, $n = 2, 3, \cdots, N-1$ and the window with maximum energy will be used as the first sampling position.

Generally, within 2 s, a person will produce respiration (exhaling or inhaling) movements and heartbeats multiple times. Therefore, choose 2 s as the base time length and step length for extraction of P times. In the first 2 s, select P starting points equally in the reference window and search backward in the slow-time direction with 2 s as the step length. In every 2 s, select and save the strongest vital sign information, then record the position of this extraction, and use this position as the reference position for the next step, until all of the P times vital signal extractions are completed. The P results obtained contain the strongest vital sign information of multiple slow time slices at different moments.

When extracting the respiration and heartbeat rates, perform FFT on the P times vital sign information extracted, find the peak value in the frequency range of respiration, and record the frequency and amplitude. Synthesize the P times results, the frequency with the most number of peaks is the respiration rate. If the number of peaks at multiple rates is the same maximum, the respiration rate will be selected which has the largest average amplitude. If the average amplitude is still the same, the frequency will be averaged. According to the above methods, the respiration rate of the trapped person can be determined; then, the one with the maximum average amplitude of all the alternative frequencies is selected as the final respiratory frequency. The vital sign information flow chart is shown in Figure 7, and the steps of the P times extraction of strong vital sign algorithm are shown in Algorithm 1.

5. Results and Discussion

5.1. Laboratory Equipment Test of the Stationary Trapped Person. The main experimental equipment is an UWB radar system based on NVA-6100 and a computer. The emission wave of this radar system is the first-order Gaussian pulse wave with a bandwidth of 0.85–9.55 GHz, which conforms to the standard of the UWB radar. The transmitting and receiving antennas of the system are both Vivaldi antennas, the gain reaches 6 dB, and the parallel distance between the two antennas is 10.2 cm. The received signal is connected to the computer through the USB; then, signal preprocessing and vital sign extraction are performed to obtain the corresponding respiration and heart rates.

A large number of tests are carried out in MATLAB, different P are performed on the received signal with a total length of 60 s, the result is obtained, when $P > 16$, and the extracted respiration and heartbeat rate values tend to be stable. Therefore, $P = 16$ is the best parameter of P times extraction of strong vital signs and the accurate vital information can be extracted in the shortest time. In the following experiment, $P = 16$ is used as the extraction standard parameter.

Name: P times extraction of strong vital signs
1) According to the signal energy, determine the initial sampling slow-time slice position and search area;
2) In the first 2 s of the area, select P extraction starting points evenly;
3) Start extraction, initialize $p = 1$;
4) Select the pth starting point to start vital signs extraction;
5) In every 2 s, select and save the strongest vital sign information, then record the extraction position, update the next reference position, until the completion of the pth extraction;
6) If $p = P$, go to step 7), otherwise $p = p + 1$, go to step 4);
7) Complete P times extraction of strong vital signs

Algorithm 1: Steps of the algorithm for P times extraction of strong vital signs.

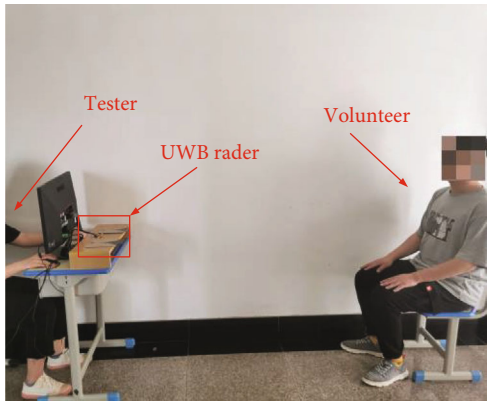

Figure 8: Experimental scene of the stationary trapped person. The radar system is placed on a table 0.85 m from the ground. The volunteer instead of the trapped person.

5.2. Test of Stationary Trapped Person. In order to verify the effectiveness and accuracy of the P times extraction of strong vital signs to the stationary trapped person, set up the experimental scene as shown in Figure 8.

The volunteer was a 26-year-old male with a height of 180 cm and a weight of 80 kg. After multiple measurements, the respiration rate of the volunteer is 0.236 Hz and the heartbeat rate is 1.081 Hz. The volunteer sits in front of the radar system with the chest cavity facing the radar system, staying still and breathing evenly. According to the above method, the volunteer sits at 1 m, 2 m, 3 m, 4 m, and 5 m away from the radar system and collects 3 sets of received signals. The 16 times extraction of strong vital signs is used on the received signals and obtains respiration and heartbeat rates. The slow time slice containing the most vital sign information is used as a comparison, and the obtained respiration rate is shown in Table 1, and the heartbeat rate is shown in Table 2.

Draw the data in Tables 1 and 2 into the graphs shown in Figures 9 and 10, where 1–3 experiments are 3 sets of data obtained by volunteers at 1 m and 4–6 experiments are the data at 2 m and so on.

The error at each distance, average error, relative, error and variance are calculated as shown in Table 3.

Combining Figure 9 and Table 3, it can be seen that for the respiration rate of the stationary volunteer at 1 m and 2 m, a single slice has a higher similarity to the volunteer's vital sign information extracted by 16 times extraction of strong vital signs. In the range of 3–5 m with weak vital sign information, the extraction effect of 16 times extraction of strong vital signs is significantly better than that of single slice. For the heartbeat rate, although the single slice extraction result can reflect volunteer's heart rate characteristics but the error is relatively larger and the error of this algorithm is smaller (see Figure 10 and Table 3).

Table 1: Respiration rate of the stationary volunteer at different distances.

Distances (m)	16 times (Hz)	Slice (Hz)	16 times (Hz)	Slice (Hz)	16 times (Hz)	Slice (Hz)
1	0.226	0.226	0.244	0.244	0.212	0.212
2	0.215	0.242	0.203	0.203	0.207	0.207
3	0.239	0.179	0.235	0.209	0.257	0.194
4	0.268	0.268	0.277	0.277	0.243	0.304
5	0.262	0.262	0.226	0.290	0.235	0.277

Table 2: Heartbeat rate of stationary volunteer at different distances.

Distances (m)	16 times (Hz)	Slice (Hz)	16 times (Hz)	Slice (Hz)	16 times (Hz)	Slice (Hz)
1	1.101	1.101	1.085	0.995	1.121	1.121
2	1.103	1.157	1.092	0.991	1.058	1.007
3	1.076	1.165	1.043	1.043	1.057	0.971
4	1.103	0.983	1.026	1.026	1.123	1.042
5	1.048	1.048	1.129	1.032	1.109	1.109

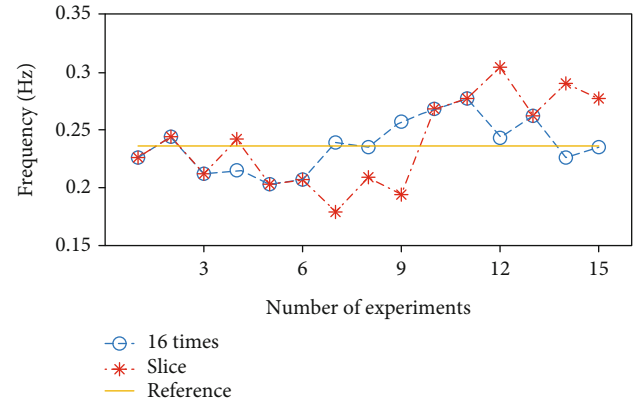

Figure 9: The respiration rate of the stationary volunteer.

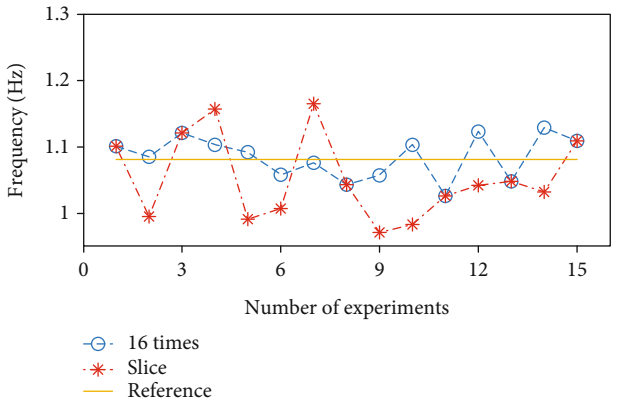

Figure 10: The heartbeat rate of the stationary volunteer.

Table 3: Error comparison of the stationary volunteer.

Error	Respiration rate		Heartbeat rate	
	16 times	Slice	16 times	Slice
Error at 1 m (Hz)	0.0140	0.0140	0.0213	0.0487
Error at 2 m (Hz)	0.0277	0.0227	0.0187	0.0800
Error at 3 m (Hz)	0.0083	0.0420	0.0223	0.0773
Error at 4 m (Hz)	0.0267	0.0470	0.0397	0.0640
Error at 5 m (Hz)	0.0123	0.0403	0.0363	0.0367
Average error (Hz)	0.0178	0.0332	0.0277	0.0613
Relative error (%)	7.54	14.07	2.56	5.64
Variance ($\times 10^{-4}$)	4.73	14.03	9.76	45.18

Table 4: Respiration rate of the micromoving volunteer at different distances.

Distances (m)	16 times (Hz)	Slice (Hz)	16 times (Hz)	Slice (Hz)	16 times (Hz)	Slice (Hz)
1 m	0.271	0.285	0.238	0.264	0.290	0.264
2 m	0.243	0.291	0.219	0.240	0.207	0.207
3 m	0.227	0.256	0.285	0.221	0.244	0.244
4 m	0.208	0.286	0.242	0.291	0.280	0.202
5 m	0.260	0.183	0.260	0.260	0.296	0.227

5.3. Test of Micromotion Trapped Person. The test of the micromoving volunteer is carried out to verify the algorithm's ability to extract signs of the micromoving trapped person. During the experiment, the volunteer moves his chest cavity slowly forward while maintaining uniform breathing and the overall moving distance was about 20 cm. According to the above measurement, the volunteer sits at 1 m, 2 m, 3 m, 4 m, and 5 m from the radar system, the respiratory rate obtained is shown in Table 4, and the heartbeat rate is shown in Table 5.

Plot the data in Tables 4 and 5 as shown in Figures 11 and 12.

Similarly, the error at each distance, average error, relative error, and variance are calculated as shown in Table 6.

Combining Figure 11 and Table 6, it can be seen that compared with the result of the stationary volunteer, the accuracy of the algorithm for extracting the respiration rate

Table 5: Heartbeat rate of the micromoving volunteer at different distances.

Distances (m)	16 times (Hz)	Slice (Hz)	16 times (Hz)	Slice (Hz)	16 times (Hz)	Slice (Hz)
1 m	1.057	0.949	1.031	1.005	1.031	0.899
2 m	1.044	1.044	1.077	0.962	1.063	0.974
3 m	1.058	0.983	1.081	0.861	1.097	0.947
4 m	1.014	0.823	1.066	0.969	0.952	0.813
5 m	1.395	1.135	1.146	0.984	1.097	0.947

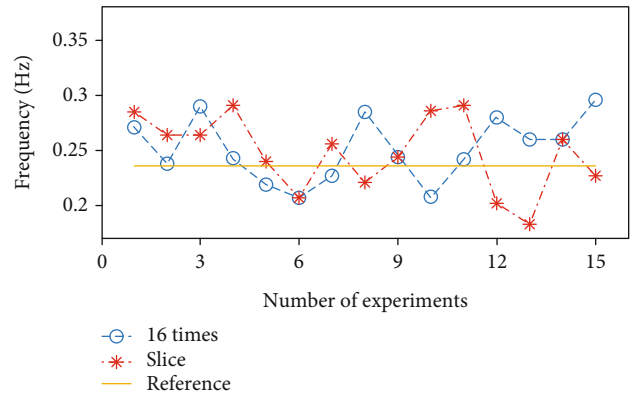

Figure 11: The respiration rate of the micromoving volunteer.

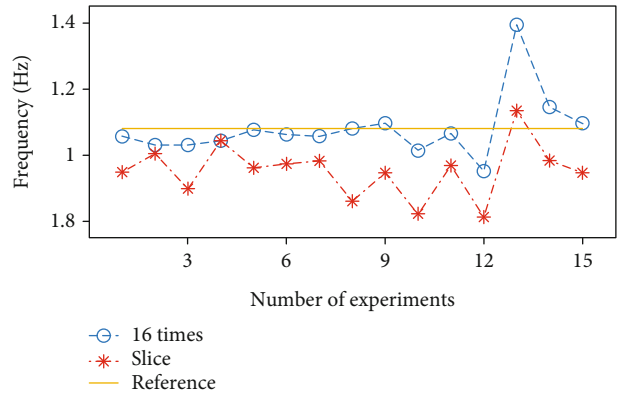

Figure 12: The heartbeat rate of the micromoving volunteer.

Table 6: Error comparison of the micromoving volunteer.

Error	Respiration rate		Heartbeat rate	
	16 times	Slice	16 times	Slice
Error at 1 m (Hz)	0.0303	0.0350	0.0413	0.1300
Error at 2 m (Hz)	0.0177	0.0293	0.0197	0.0877
Error at 3 m (Hz)	0.0220	0.0143	0.0130	0.1507
Error at 4 m (Hz)	0.0260	0.0463	0.0703	0.2127
Error at 5 m (Hz)	0.0360	0.0287	0.1317	0.0950
Average error (Hz)	0.0264	0.0307	0.0552	0.1352
Relative error (%)	11.19	13.01	5.11	12.51
Variance ($\times 10^{-4}$)	10.25	12.46	88.34	226.98

of the micromoving volunteer has decreased but it is still better than the single slice.

Combining Figure 12 and Table 6, it can be seen that the respiration rate obtained by a single slice is basically below the reference value and the average error is relatively larger. The extraction result of this algorithm is basically stable near the reference value and only has a significant error at the position of 4–5 m.

5.4. Performance Comparison. As the results shown in Tables 1–6, for stationary trapped persons, the relative error of the respiration rate extracted by this method is 7.54% and the relative error of heartbeat rate is 2.56%, which are better than the result of single slice. Because of the movement of the micromovement trapped person, the results of respiration and heartbeat rates have a larger error. However, compared with the extraction results of a single slice, the relative errors of respiratory and heartbeat rate extraction results of this algorithm are reduced by 1.82% and 7.3%, respectively. And the variance of this algorithm is smaller than that of single slice results in all comparisons, which can reflect that this algorithm has better stability.

6. Conclusions

In this paper, a new vital sign detection algorithm based on the UWB radar is proposed. This method parses different noise interferences by the cumulative probability density and uses linear error correction, linear trend suppression, and signal enhancement to realize the preprocessing. The region of the trapped person is judged by the energy of the processed signal, and P times of extraction is used to obtain the strongest vital sign. Then, the respiration and heartbeat rates were determined by the distribution of the peak from the P group frequency spectrum. Experimental data show that this method can more accurately determine the respiration and heartbeat rates of the stationary trapped person and has a better performance for the micromoving one.

Data Availability

The test data used to support the findings of this study are available from the corresponding author upon request.

Conflicts of Interest

The authors declared that they have no conflicts of interest to this work. We declare that we do not have any commercial or associative interest that represents a conflict of interest in connection with the work submitted.

Acknowledgments

The author thanks the entire team for their contributions to the paper. This work is supported by the discipline innovation team of Liaoning Technical University (LNTU20TD-29) and Liaoning Educational Committee Foundation (nos. LJ2019JL013 and LJ2020JCL020).

References

[1] S. D. Liang, "Sense-through-wall human detection based on UWB radar sensors," *Signal Processing*, vol. 126, pp. 117–124, 2016.

[2] L. Liu, Z. Liu, H. Xie, B. Barrowes, and A. Bagtzoglou, "Numerical simulation of UWB impulse radar vital sign detection at an earthquake disaster site," *Ad Hoc Networks*, vol. 13, pp. 34–41, 2014.

[3] L. B. Jiang, C. Li, and L. Che, "Human motion recognition using ultra-wide band radar based on two-dimensional wavelet packet decomposition," *Journal of Electronic Measurement and Instrumentation*, vol. 32, no. 8, pp. 69–75, 2018.

[4] Y. Zhang, T. Jiao, X. J. Jing, H. Wang, X. Yu, and J. Q. Wang, "Current state and progress of the technology of bioradar," *Informatization Research*, vol. 36, no. 10, pp. 6–10+13, 2010.

[5] X. Y. Liu, H. R. Cui, Z. Liu, Y. Z. Zhu, T. Liu, and Y. W. Wang, "Detection of human body signs based on Doppler radar sensor," *Transducer and Microsystem Technologies*, vol. 39, no. 5, pp. 137–139, 2020.

[6] Y. Zhang, F. Qi, H. Lv, F. Liang, and J. Wang, "Bioradar technology: recent research and advancements," *IEEE Microwave Magazine*, vol. 20, no. 8, pp. 58–73, 2019.

[7] C. Cui and Q. Zhao, "Design of vital signs detection system based on micro-Doppler radar," *Control Engineering of China*, vol. 26, no. 1, pp. 105–107, 2019.

[8] S. Dai, F. Zhu, Y. Y. Xu, and G. Y. Fang, "Vital signal detection method based on principal component analysis and empirical mode decomposition for ultra wideband radar," *Acta Electronica Sinica*, vol. 40, no. 2, pp. 344–349, 2012.

[9] J. H. Zhou, Y. C. Wang, J. P. Tong, S. Y. Zhou, and X. F. Wu, "Ultra wide band radar gait recognition based on slow-time segmentation," *Journal of Zhejiang University (Engineering Science)*, vol. 54, no. 2, pp. 283–290, 2020.

[10] S. Wu, K. Tan, Z. Xia, J. Chen, S. Meng, and F. Guangyou, "Improved human respiration detection method via ultra-wideband radar in through-wall or other similar conditions," *IET Radar, Sonar & Navigation*, vol. 10, no. 3, pp. 468–476, 2016.

[11] J. Li, Z. Zeng, J. Sun, and F. Liu, "Through-wall detection of human being's movement by UWB radar," *Geoscience and Remote Sensing Letters*, vol. 9, no. 6, pp. 1079–1083, 2012.

[12] Y. Xu, S. Dai, S. Wu, J. Chen, and G. Fang, "Vital sign detection method based on multiple higher order cumulant for ultrawideband radar," *IEEE Transactions on Geoscience and Remote Sensing*, vol. 50, no. 4, pp. 1254–1265, 2012.

[13] A. Nezirovic, A. G. Yarovoy, and L. P. Ligthart, "Signal processing for improved detection of trapped victims using UWB radar," *IEEE Transactions on Geoscience and Remote Sensing*, vol. 48, no. 4, pp. 2005–2014, 2010.

[14] F. M. Shikhsarmast, T. Lyu, X. Liang, H. Zhang, and T. Gulliver, "Random-noise denoising and clutter elimination of human respiration movements based on an improved time window selection algorithm using wavelet transform," *Sensors (Basel)*, vol. 19, no. 1, p. 95, 2019.

[15] G. C. Yang and H. M. Yu, "Vital sign detection of ultra-wideband radar based on N peaks capture," *Journal of Electronic Measurement and Instrumentation*, vol. 34, no. 11, pp. 204–210, 2020.

[16] B. Li, W. W. Fu, and Y. Wang, "Signal processing for ultra-wideband life detection radar based on periodic sampling,"

Chinese Journal of Scientific Instrument, vol. 31, no. 9, pp. 1979–1985, 2010.

[17] J. Li, L. Liu, Z. Zeng, and F. Liu, "Advanced signal processing for vital sign extraction with applications in UWB radar detection of trapped victims in complex environments," *IEEE Journal of Selected Topics in Applied Earth Observations and Remote Sensing*, vol. 7, no. 3, pp. 783–791, 2014.

[18] G. Zhao, Q. Liang, and T. S. Durrani, "An EMD based sense-through-foliage target detection UWB radar sensor networks," *IEEE Access*, vol. 6, pp. 29254–29261, 2018.

[19] X. Liang, H. Zhang, S. Ye, G. Fang, and T. Aaron Gulliver, "Improved denoising method for through-wall vital sign detection using UWB impulse radar," *Digital Signal Processing: A Review Journal*, vol. 74, pp. 72–93, 2018.

[20] K. Shyu, L. Chiu, P. Lee, T. Tung, and S. Yang, "Detection of breathing and heart rates in UWB radar sensor data using FVPIEF-based two-layer EEMD," *IEEE Sensors Journal*, vol. 19, no. 2, pp. 774–784, 2019.

[21] T. Zhou, G. Cai, M. Lin et al., "A modified two-dimension EEMD method for breathing and heart rates monitoring via through-wall IR-UWB radar," in *International Symposium on Medical Information and Communication Technology*, vol. 15pp. 41–46, Xiamen, China, 2021.

[22] L. Liu, Z. Liu, and B. E. Barrowes, "Through-wall bio-radiolocation with UWB impulse radar: observation, simulation and signal extraction," *IEEE Journal of Selected Topics in Applied Earth Observations and Remote Sensing*, vol. 4, no. 4, pp. 791–798, 2011.

[23] A. Lazaro, D. Girbau, and R. Villarino, "Techniques for clutter suppression in the presence of body movements during the detection of respiratory activity through UWB radars," *Sensor*, vol. 14, no. 2, pp. 2595–2618, 2014.

[24] S. Wu, S. Yao, W. Liu et al., "Study on a novel UWB linear array human respiration model and detection method," *IEEE Journal of Selected Topics in Applied Earth Observations and Remote Sensing*, vol. 9, no. 1, pp. 125–140, 2016.